NASA Technical Paper 3300

February 1993

Mars Surface Radiation Exposure for Solar Maximum Conditions and 1989 Solar Proton Events

Lisa C. Simonsen
and John E. Nealy

NASA Technical Paper 3300

1993

Mars Surface Radiation Exposure for Solar Maximum Conditions and 1989 Solar Proton Events

Lisa C. Simonsen
and John E. Nealy
Langley Research Center
Hampton, Virginia

Abstract

The Langley heavy-ion/nucleon transport code, HZETRN, and the high-energy nucleon transport code, BRYNTRN, are used to predict the propagation of galactic cosmic rays (GCR's) and solar flare protons through the carbon dioxide atmosphere of Mars. Particle fluences and the resulting doses are estimated on the surface of Mars for GCR's during solar maximum conditions and the August, September, and October 1989 solar proton events. These results extend previously calculated surface estimates for GCR's at solar minimum conditions and the February 1956, November 1960, and August 1972 solar proton events. Surface doses are estimated with both a low-density and a high-density carbon dioxide model of the atmosphere for altitudes of 0, 4, 8, and 12 km above the surface. A solar modulation function is incorporated to estimate the GCR dose variation between solar minimum and maximum conditions over the 11-year solar cycle. By using current Mars mission scenarios, doses to the skin, eye, and blood-forming organs are predicted for short- and long-duration stay times on the Martian surface throughout the solar cycle.

Introduction

For a successful human Mars mission, the anticipated radiation doses incurred by crew members and subsequent shielding estimates must be assessed both in free space and on the Mars surface. The largest doses will most likely be encountered in transit to and from Mars. Relief from the harsh free-space radiation environment, including galactic cosmic rays (GCR's) and solar proton flares, can be found on the surface of Mars. Unlike Earth, Mars is devoid of an intrinsic magnetic field allowing many of the free-space high-energy charged particles to reach the outer atmosphere. However, the carbon dioxide atmosphere of Mars will attenuate the charged particle fluxes and provide a significant amount of protection.

The analysis presented here addresses the possible doses to crew members while on the Martian surface. New dose estimates are presented for GCR's at solar maximum conditions and the August, September, and October 1989 solar proton events. This analysis extends previously estimated doses incurred from GCR's at solar minimum conditions and the February 1956, November 1960, and August 1972 flare events (Simonsen et al. 1990a). The 1989 flares are typical of the rarely occurring large flares, while the smaller normally occurring flares are much less hazardous. These smaller flares do not contribute significantly to dose on the surface of Mars because of the relatively large amount of atmospheric protection. The galactic cosmic rays are also a source of exposure characterized by a much lower but continuous dose rate. The contribution to dose from GCR's varies with the 11-year solar cycle, and the largest contribution occurs during solar minimum conditions. The GCR contribution becomes more important as the mission duration increases.

Both short and long stay times on the surface are considered throughout the 11-year solar cycle. Dose estimates are calculated for short stay times on the order of 30, 60, and 90 days after a 7-month to 1-year transit flight. An unexpected flare event that occurs while the crew is on the surface may contribute significantly to these total mission dose estimates. Longer stay times of $\approx$400–600 days when the GCR dose dominates are also considered.

Symbols and Abbreviations

AU	astronomical unit
BFO	blood-forming organ
BRYNTRN	baryon transport code
COSPAR	Committee on Space Research
CREME	cosmic ray effects on microelectronics
c	number density (particles/volume)
Gray	1 Gy = 100 rad, 1 cGy = 1 rad
GCR	galactic cosmic ray
GOES-7	Geostationary Operational Environmental Satellite
H	dose-equivalent rate
HZETRN	heavy-ion/nucleon transport code
h	altitude above Martian surface

LEO	low Earth orbit
LET	linear energy transfer
M	molecular weight
MIRACAL	Mission Radiation Calculation program
N_A	Avogadro's number
NCRP	National Council on Radiation Protection and Measurements
R	radius of Mars
r	distance from Sun
Sievert	1 Sv = 100 rem, 1 cSv = 1 rem
s	distance along slant path
t	time after last solar minimum
$w(t)$	modulation function value
Z	atomic number
z	vertical altitude
θ	zenith angle
T	absorber linear density

Radiation Exposure

Currently, radiation-exposure limits are not established for an exploratory-class Mars mission. However, the National Council on Radiation Protection and Measurements (NCRP) recommends that the limits established for low Earth orbit (LEO) operations be used as guidelines if the principle of ALARA (as low as reasonably achievable) is followed (Anon. 1989). LEO limits are established for the skin, ocular lens, and blood-forming organs as shown in table 1. For high-energy radiation from GCR's and solar proton flares, the dose delivered to the vital organs is the most important with regard to latent carcinogenic effects. This dose is often considered to be the whole-body exposure and is referred to as the blood-forming organ (BFO) dose.

When detailed body geometry is not considered, the BFO dose is usually computed as the dose incurred at a 5-cm depth in tissue (simulated in this analysis by water). A conservative estimate for the skin and eye dose is made with the 0-cm-depth dose. Dose-equivalent limits are established for the short-term (30-day) exposures, annual exposures, and career exposures for astronauts in low Earth orbit. The short-term exposures are important when considering solar flare events because of their high dose rate.

Table 1. Ionizing Radiation Exposure Limits for LEO

[Data from NCRP-98 (Anon. 1989)]

Exposure interval	Dose equivalent, cSv		
	Blood-forming organ	Ocular lens	Skin
30-day	25	100	150
Annual	50	200	300
Career	[a]100–400	400	600

[a]Varies with gender and age at initial exposure.

Doses received from GCR's on long-duration missions are especially important to total career limits, which are determined by the age and gender of the individual.

The dose-equivalent limits are included in this paper only for discussion purposes. Exploratory-class missions will most likely receive separate consideration (Anon. 1989). In addition, the surface doses are the only portion of the mission addressed in this paper. Large doses may be received while in transit from GCR's, solar proton events, and the Van Allen belts. (See Nealy, Simonsen, and Striepe 1992; Simonsen and Nealy 1991; Striepe, Nealy, and Simonsen 1992; Striepe, Simonsen, and Nealy 1992; Townsend et al. 1989 and 1992; Townsend, Shinn, and Wilson 1991; Townsend, Cucinotta, and Wilson 1992.) Human-made nuclear sources (e.g., nuclear-powered propulsion) must also be addressed when applicable (Nealy et al. 1991), and the total mission dose should be compared with the guideline constraints.

Radiation Environment

The free-space radiation environment varies over the 11-year solar cycle. At solar minimum conditions, the interplanetary magnetic field is weakest and thus allows more intergalactic particles to gain access to our solar system. Thus, the GCR fluxes and the incurred doses from GCR's are the greatest during solar minimum conditions. During solar maximum conditions, the GCR fluxes are lowest; however, the probability of a large solar proton event increases significantly. The solar flare rate of occurrence is greatest between the third and ninth years after the last solar minimum (i.e., years 3 to 9 in the solar cycle; Nealy, Striepe, and Simonsen 1992). Solar cycle XXII spans approximately the years of 1986 to 1996, and the solar maximum for this cycle occurs around 1989 to 1994. Many of the current Mars mission scenarios are scheduled during solar cycle XXIV ($\approx$2007–2018) and solar cycle XXV ($\approx$2018–2029).

Galactic Cosmic Radiation

Galactic cosmic radiation consists of the nuclei of the chemical elements that have been accelerated to extremely high energies outside the solar system. The natural GCR environment used in this analysis is the widely used Naval Research Laboratory CREME model, which specifies ion fluxes for particles of atomic numbers between 1 and 28 (hydrogen through nickel, Adams, Silberberg, and Tsao 1981). Figure 1 shows the GCR particle spectra at solar minimum conditions; considerable uncertainty exists in the energy distribution of these ions. At solar maximum conditions, GCR fluxes are substantially reduced. Figure 2 shows the amount of flux reductions for the various species groups in terms of the energy-dependent ratios of solar maximum to solar minimum fluxes (Adams, Silberberg, and Tsao 1981). The flux reduction is most pronounced for the energy range between 1 and 10^3 MeV, while the particles of higher energies (greater than 10^4 MeV) are only slightly affected by solar cycle variation.

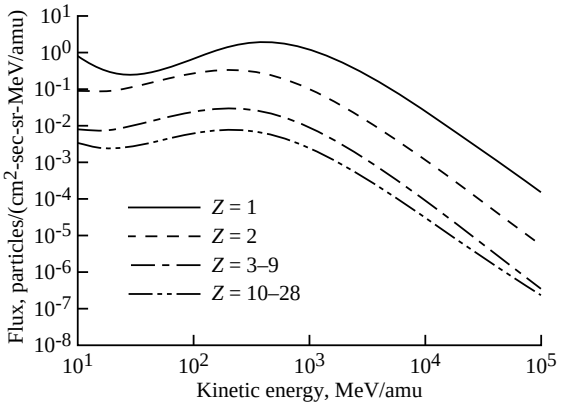

Figure 1. Galactic cosmic ray differential flux spectra at solar minimum for selected elemental groups.

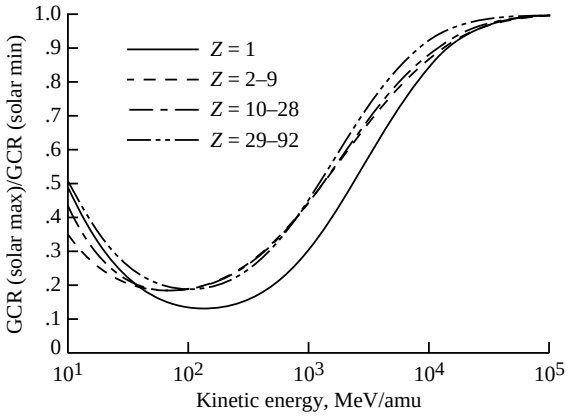

Figure 2. Ratios of galactic cosmic ray differential flux at solar maximum to corresponding flux at solar minimum for selected elemental groups.

The flux variation between the cycle extrema is calculated with a weighting or modulation function that determines the fractional solar minimum to solar maximum fluxes observed at a given time within the cycle. The modulation of the GCR flux depends directly on the intensity of the solar activity. Solar activity can be gauged by examining the intensity of the 10.7-cm microwave flux (F10.7 index), which is somewhat less sporadic than other indices (e.g., sunspot number, magnetic indices, and ground-based neutron monitors). The modulation function of figure 3 was derived from the F10.7 index variation during solar cycle XXI (Withbroe 1989).

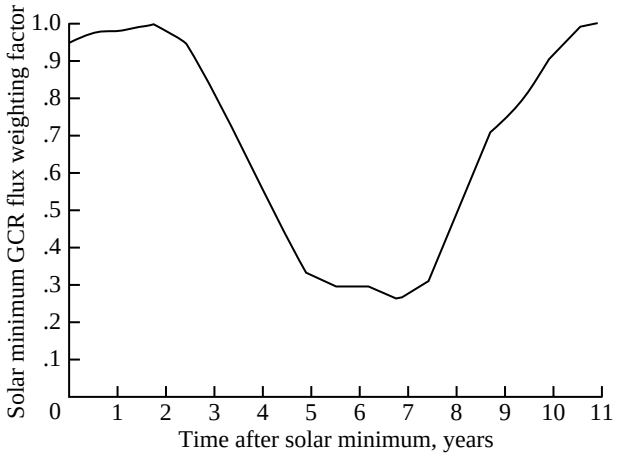

Figure 3. Modulation function for GCR flux as derived for solar cycle XXI in terms of the weighting factor for observed peak (solar minimum) flux.

The modulation represents the reduction factor to be applied to the peak GCR flux as a function of time throughout the 11-year cycle. This weighting function has a reciprocal relationship with the magnitude of the 10.7-cm flux, which characteristically is observed to return to approximately the same level at solar minimum for each cycle. However, during solar maximum, levels of solar activity are observed to vary from cycle to cycle. Because solar cycle XXI was a relatively weak cycle during active Sun years, GCR fluxes in the present model never attain their minimum values. Consequently, some degree of conservatism is present in the modeled GCR fluxes. The actual solar minimum fluxes have been observed to exhibit a time lag relative to the 10.7-cm flux (Smart and Shea 1989); an improved modulation function would incorporate a phase delay of 8 to 12 months.

Solar Proton Flares

Large solar flare events are relatively rare; however, they are potentially dangerous. They can deliver high dose rates to insufficiently shielded crew members. Except for the near certainty that such events occur during the years of solar maximum, large flares are practically unpredictable with regard to their time of occurrence and spectral characteristics. Recently, several flares that were larger than any recorded since the August 1972 event occurred in the months of August through December 1989. These flares were recorded by the GOES-7 satellite and include the August 12, September 29, and October 19, 1989 flares. Figure 4 shows the proton fluence energy spectra based on rigidity functions reported by Sauer, Zwickl, and Ness (1990). The addition of the three 1989 flare events provides a fairly realistic estimate of a flare environment that can be encountered during missions occurring in the 5 or 6 years of active Sun conditions.

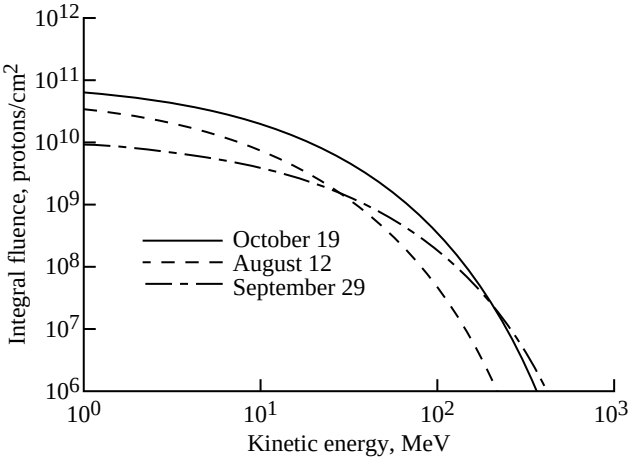

Figure 4. Three large solar flare fluences for 1989 solar proton events; graph based on GOES-7 data.

Martian Atmosphere

The Martian atmosphere provides protection from GCR's and solar flares. The composition of the lower atmosphere by volume is approximately 95.3 percent carbon dioxide, 2.7 percent nitrogen, and 1.6 percent argon (Smith and West 1983). For the present analysis, the atmosphere is assumed to be 100 percent carbon dioxide. The Committee on Space Research (COSPAR) has used atmospheric structure data gathered during the Viking entries to develop the COSPAR warm, high-density atmosphere model and the COSPAR cool, low-density atmosphere model. These models use the daily mean temperatures and pressures at midlatitude sites during the summer season (Smith and West 1983). Figure 5 shows the vertical pressure profile. The low-density model assumes a surface pressure of 5.9 mbar and provides approximately 16 g/cm^2 of carbon dioxide shielding in the vertical direction. The high-density model assumes a surface pressure of 7.8 mbar and provides 22 g/cm^2 of carbon dioxide in the vertical direction.

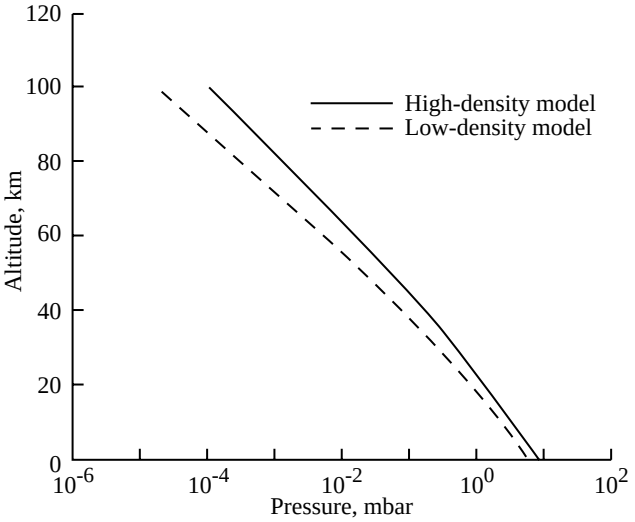

Figure 5. COSPAR vertical pressure profile of Martian atmosphere model.

The amount of protection provided by the atmosphere varies seasonally as the surface pressure on Mars varies. Pressures varied at the Viking I and Viking II landing sites by approximately 2.0 to 2.5 mbar. Viking I varied between 6.8–9.0 mbar, and Viking II varied between 7.5–10.0 mbar (Hess et al. 1980). The altitude of the site also affects the amount of shielding provided. Table 2 shows the decreasing amount of protection provided by the atmosphere in the vertical direction at increasing altitudes. Dose estimates at altitudes up to 12 km are included in the analysis because of the great deal of topographical relief present on the Mars surface. The two atmosphere models are considered to provide a reasonable estimate of the possible variation in the radiation intensities found at the surface.

Table 2. Mars Atmospheric Protection in the Vertical Direction

Altitude, km	Protection, g/cm^2 CO_2	
	Low-density model	High-density model
0	16	22
4	11	16
8	7	11
12	5	8

Transport and Dosimetry Analysis

The transport of high-energy nucleons and heavy ions through condensed matter is calculated with two nucleon codes developed at Langley: BRYNTRN (Wilson et al. 1989) and HZETRN (Wilson et al. 1991a). Both codes implement combined numerical and analytical techniques to provide solutions to the one-dimensional Boltzmann transport equation for particle flux and energy. The BRYNTRN code transports primary and secondary nucleons and includes the effects of target nucleus recoil reactions. The energy loss by heavy target fragments and recoil nuclei is assumed to be deposited locally. The present calculations are performed for the flare input proton spectrum through use of a logarithmic energy grid between 0.01 and 3000 MeV. The GCR calculations are performed with the HZETRN code, which transports nuclear species with charge numbers between 0 and 28. Secondary products from nuclear fragmentation reactions are also transported. The energy grid of 160 points is logarithmic over a range between 0.01 and 128 000 MeV.

Both BRYNTRN and HZETRN evaluate dosimetric quantities based on the linear energy transfer of particles traversing the media. The dose is evaluated in terms of cGy or rads (100 ergs/g). For human exposure, the dose equivalent (in terms of cSv or rem) is defined by introducing the quality factor that relates the biological risk produced because of any ionizing radiation to the damage produced by soft X-rays. In general, the quality factor is a function of linear energy transfer (LET), which in turn is a function of particle type and energy. For the present calculations, the quality factors used are those specified by the International Commission on Radiological Protection (Anon. 1987). Although HZE (high charge and energy) particles are present in the GCR fluxes and to a lesser extent in the nuclear reaction products of GCR and solar flare protons (Anon. 1989), their biological effects are not well understood and lead to uncertainty in risk estimates (Cucinotta et al. 1991). Thus, the definition of new quality factors relating dose to biological damage may impact the present results. In addition to the previous references for the nucleon codes, the reference publication by Wilson et al. (1991b) provides great detail on space radiation transport methodology and analysis.

Transport Computational Results

The HZETRN and BRYNTRN nucleon codes are used to generate dose data for the initial particle fluxes through carbon dioxide. The flux-energy distributions as previously described for the modulated GCR's and the 1989 proton flares are used as input. The calculated slab-dose results correspond to a monodirectional beam of particles normally incident on a planar layer of shield material.

Galactic Cosmic Radiation

Figures 6 and 7 show the skin and BFO dose and dose-equivalent rates as a function of CO_2 absorber amount for GCR's at solar maximum conditions. The BFO results represent the dose evaluated after traversing a given absorber amount of CO_2 with an additional 5-cm tissue layer (water). The difference between the corresponding skin and BFO doses represents the body's self-shielding. Although the code simulates the transport of particles 0, 1, 2, ..., 28 individually, the dose contributions are represented as five entities for illustration: (1) neutrons, (2) protons, (3) alpha particles, (4) lighter nuclei ($3 \leq Z \leq 9$), and (5) heavier nuclei ($10 \leq Z \leq 28$). The higher dose-equivalent values illustrate the impact of the quality factors on the biological damage incurred. The protons dominate the dose through 100 g/cm^2 of CO_2; however, the heavy ions ($10 \leq Z \leq 28$) dominate the dose equivalent through approximately the first 20 g/cm^2 because of their high quality factors.

1989 Solar Proton Events

Figures 8 and 9 show the skin and BFO dose and dose equivalent as a function of CO_2 absorber amount for the 1989 solar proton events. The difference between the dose and the dose equivalent is smaller for the solar flare spectra than for the GCR spectra because of the high-quality factors associated with the heavy-ion GCR constituents. The solar flares also attenuate much more rapidly by CO_2 than do the GCR's because of the absence of high-energy particles in the GCR spectrum. Compared with the August and September flares, the October 1989 flare delivers the largest dose at the surface because of its generally larger fluxes at higher energies. This result is further exemplified by the dose-depth curves, which show that the October event delivers the largest dose of the three flares at equal absorber thicknesses. After approximately 25 g/cm^2, the doses of all three flares approach levels that do not impose a short-term (acute) hazard.

Dose Estimates on Martian Surface

The surface doses at various altitudes in the Mars atmosphere are determined from the computed

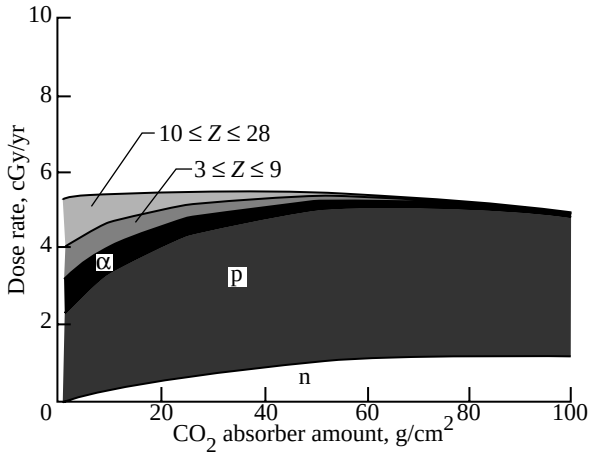

(a) Skin dose.

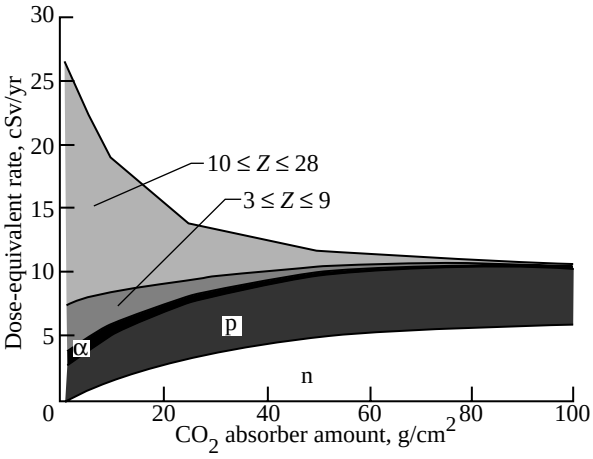

(b) Skin dose equivalent.

Figure 6. Annual skin dose and dose-equivalent contributions from specified particle constituents as a function of CO_2 absorber amount for GCR at solar maximum conditions.

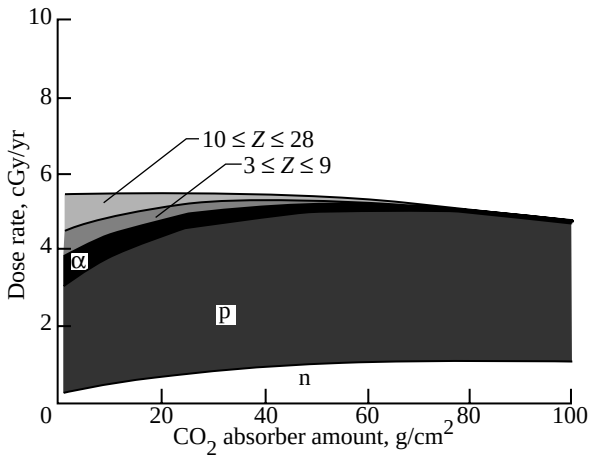

(a) BFO dose.

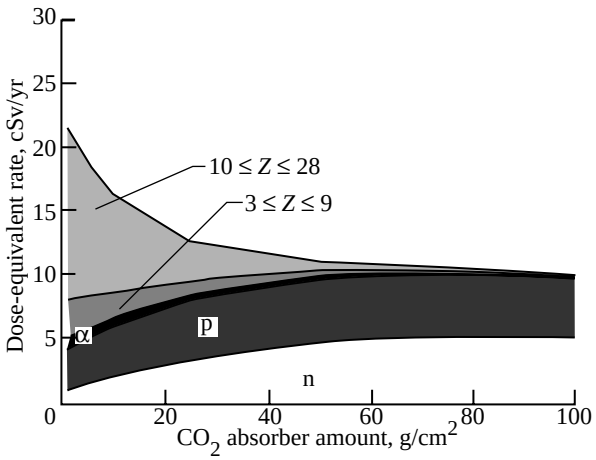

(b) BFO dose equivalent.

Figure 7. Annual BFO dose and dose-equivalent contributions from specified particle constituents as a function of CO_2 absorber amount for GCR at solar maximum conditions.

propagation data for the GCR's and solar flare protons. The dosimetric values at a given target point are computed for CO_2 absorber amounts along slant paths through the atmosphere. As shown in figure 10, a spherically concentric atmosphere model is assumed. For a target point at altitude h above the surface, the distance s along a slant path with zenith angle θ is given by

$$s(z,\theta) = \sqrt{(R+h)^2\cos^2\theta + \left[2R(z-h) + z^2 - h^2\right]} - (R+h)\cos\theta$$

where z is the vertical altitude and R is the radius of Mars. The absorber amount T along the slant path in g/cm^2 is then

$$T(h,\theta) = \frac{M_{CO_2}}{N_A}\int_0^\infty c(s)\,ds$$

where M is the molecular weight and c is the number density. For a given target point, the absorber amounts and the corresponding dosimetric quantities are evaluated for zenith angles between 0° and 90° in increments of 5°. For example, on the surface (0 km) at a zenith angle of 0°, the low-density model provides 16.0 g/cm^2 of protection, and the protection increases to 59.6 g/cm^2 at 75°. The dose and dose equivalents corresponding to each absorber thickness at each zenith angle are interpolated or extrapolated from the basic dose-depth propagation data. The calculated directional dose is then numerically integrated over a solid angle of 2π to obtain the total dose at the point of interest. (The dose from the other solid angle of 2π is assumed to be zero because of planetary shielding.)

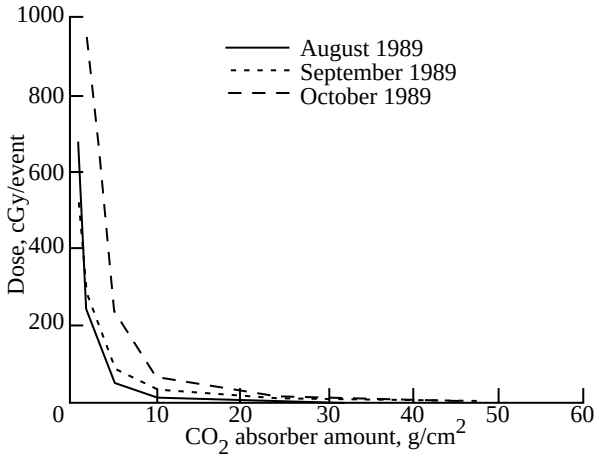

(a) Skin dose.

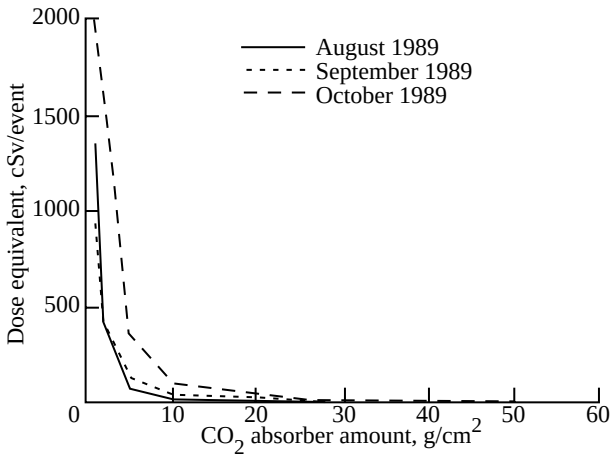

(b) Skin dose equivalent.

Figure 8. Skin dose and dose-equivalent as a function of CO_2 absorber amount for three 1989 solar proton events.

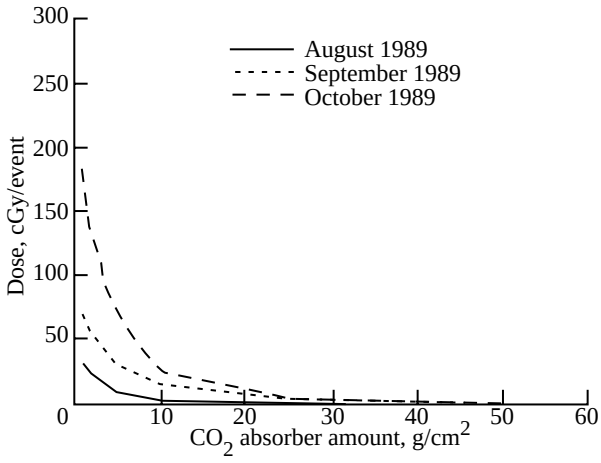

(a) BFO dose.

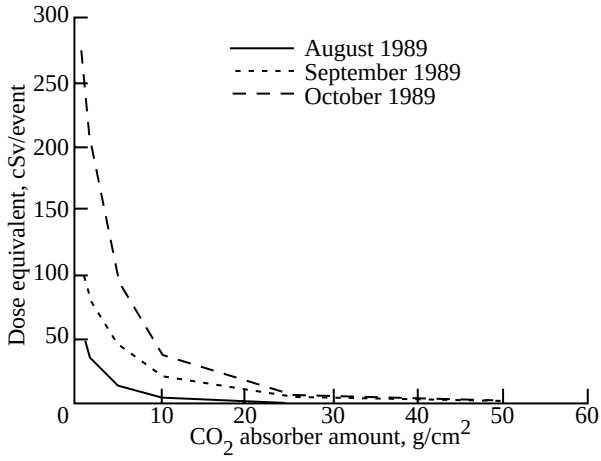

(b) BFO dose equivalent.

Figure 9. BFO dose and dose equivalent as a function of CO_2 absorber amount for three 1989 solar proton events.

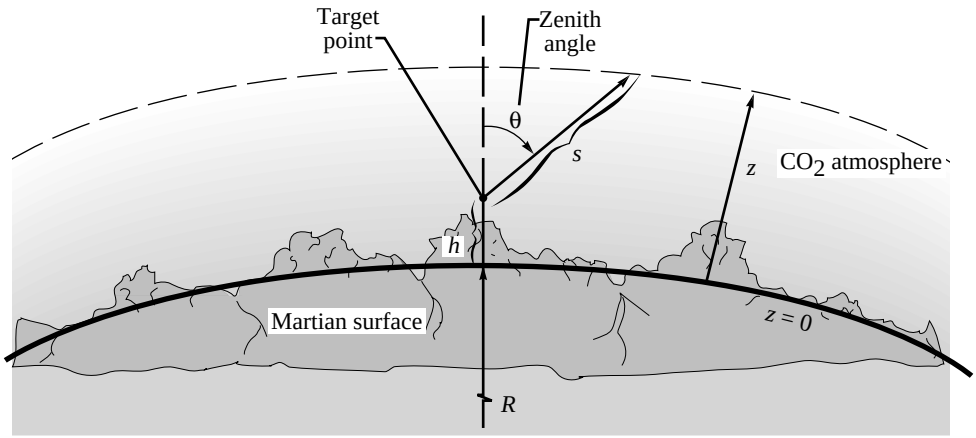

Figure 10. Martian atmosphere geometry and parameters associated with dose calculations at target point.

Table 3. Integrated Dose for Mars High-Density Atmosphere Model

Radiation source	Exposure location	Integrated dose, cGy, at altitude of— 0 km	4 km	8 km	12 km
GCR at solar minimum (annual)	Skin	5.3	5.7	6.1	6.4
	BFO	5.1	5.5	5.9	6.2
GCR at solar maximum (annual)	Skin	2.6	2.7	2.7	2.8
	BFO	2.5	2.6	2.7	2.8
August 1989 flare event	Skin	0.1	0.3	0.9	2.3
	BFO	0.1	0.2	0.4	0.8
September 1989 flare event	Skin	1.0	2.3	4.5	8.4
	BFO	0.7	1.4	2.6	4.3
October 1989 flare event	Skin	1.2	3.3	7.9	17.1
	BFO	0.8	1.8	3.8	7.2

Table 4. Integrated Dose Equivalent for Mars High-Density Atmosphere Model

Radiation source	Exposure location	Integrated dose equivalent, cGy, at altitude of— 0 km	4 km	8 km	12 km
GCR at solar minimum (annual)	Skin	11.3	13.4	15.8	18.6
	BFO	10.5	12.0	13.7	15.6
GCR at solar maximum (annual)	Skin	6.2	6.8	7.5	8.3
	BFO	5.7	6.2	6.7	7.3
August 1989 flare event	Skin	0.2	0.5	1.4	3.6
	BFO	0.1	0.3	0.6	1.2
September 1989 flare event	Skin	1.5	3.3	6.6	12.3
	BFO	1.0	2.0	3.7	6.1
October 1989 flare event	Skin	1.9	5.1	11.8	25.6
	BFO	1.2	2.8	5.7	10.6

Table 5. Integrated Dose for Mars Low-Density Atmosphere Model

Radiation source	Exposure location	Integrated dose, cGy, at altitude of— 0 km	4 km	8 km	12 km
GCR at solar minimum (annual)	Skin	5.7	6.1	6.5	6.8
	BFO	5.5	5.9	6.2	6.5
GCR at solar maximum (annual)	Skin	2.7	2.7	2.8	2.8
	BFO	2.6	2.7	2.8	2.8
August 1989 flare event	Skin	0.3	0.9	2.6	6.8
	BFO	0.1	0.4	0.9	1.7
September 1989 flare event	Skin	2.1	4.7	9.1	17.2
	BFO	1.4	2.6	4.6	7.4
October 1989 flare event	Skin	3.2	8.2	18.9	41.6
	BFO	1.7	4.0	7.8	14.1

Table 6. Integrated Dose Equivalent for Mars Low-Density Atmosphere Model

Radiation source	Exposure location	Integrated dose equivalent, cGy, at altitude of— 0 km	4 km	8 km	12 km
GCR at solar minimum (annual)	Skin	13.2	15.9	18.9	22.4
	BFO	11.9	13.8	15.8	18.0
GCR at solar maximum (annual)	Skin	6.7	7.6	8.4	9.4
	BFO	6.1	6.8	7.4	8.1
August 1989 flare event	Skin	0.5	1.5	4.0	10.7
	BFO	0.3	0.6	1.3	2.6
September 1989 flare event	Skin	3.1	6.8	13.3	25.5
	BFO	2.0	3.8	6.5	10.6
October 1989 flare event	Skin	4.8	12.3	28.2	63.3
	BFO	2.7	5.9	11.4	20.5

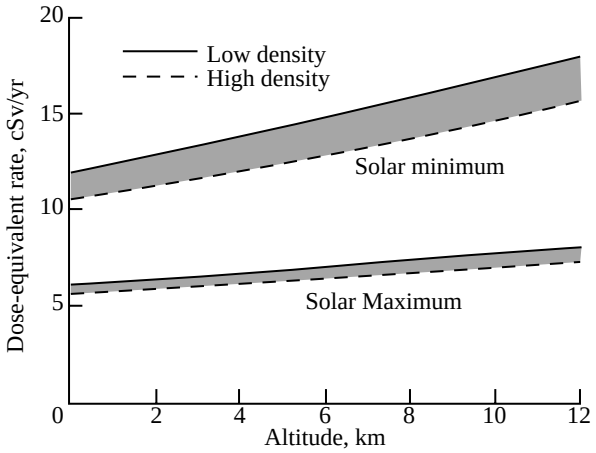

Figure 11. GCR BFO dose equivalent for solar minimum and maximum conditions as a function of altitude.

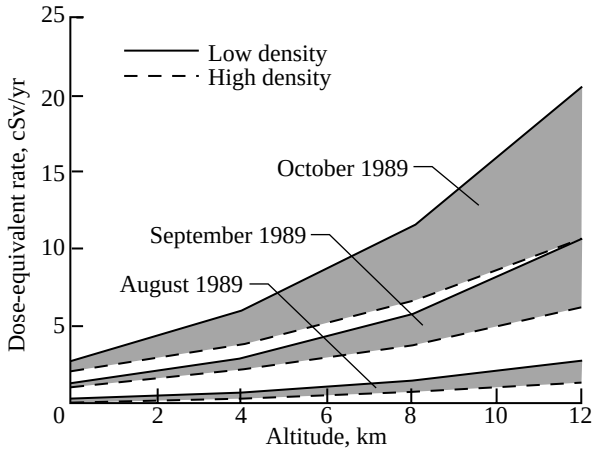

Figure 12. BFO dose equivalent for August, September, and October 1989 flares as a function of altitude.

Integrated dose and dose-equivalent calculations are made for both the high-density and the low-density atmosphere models at altitudes of 0, 4, 8, and 12 km. Tables 3 to 6 show the results, which include dose estimates for the GCR at solar maximum conditions and the 1989 solar proton events. In addition, previously calculated GCR doses at solar minimum are included (Simonsen et al. 1990a). Dose estimates for the February 1956, November 1960, and August 1972 solar proton events can be found in the report by Simonsen et al. (1990a). As shown in tables 3 to 6, the incurred GCR dose during solar maximum conditions (5.68–6.14 cSv/yr BFO) is approximately half of the dose incurred during solar minimum conditions (10.5–11.9 cSv/yr BFO). Compared with the range of estimated flare doses, the GCR remains relatively constant with altitude. The variation of BFO dose equivalent with altitude is illustrated in figures 11 and 12, which can be used to estimate dose levels at altitudes other than those listed in tables 3 to 6. Of the 1989 flares, the October flare delivers the greatest dose equivalent; it ranges from 1.21- to 20.51-cSv BFO at altitudes of 0 and 12 km, respectively.

The flare doses are estimated with the fluence at 1 AU. In the vicinity of Mars ($\approx$1.5 AU), the fluence of these flares is expected to be less. A reasonable estimate is that the radial dispersion of the flare particle flux is inversely proportional to the square of the distance from the Sun (Anon. 1975). However, large variabilities in this behavior are expected primarily because of inhomogeneities in the interplanetary magnetic field, anisotropic flux properties, and the nature of the energy spectrum (Svestka 1976). The reader must decide whether the estimated flare doses should be multiplied by $1/r^2$ (where for Mars, the distance from the Sun, r, is about 1.5 AU).

Mission Dose Estimates

The values in tables 7 and 8 are used to estimate the total dose incurred while on the surface of Mars during a variety of proposed missions occurring at various times during the solar cycle. The GCR dose variation over the 11-year solar cycle can be evaluated with the modulation function previously described. The GCR dose-equivalent rate H_{GCR} at time t (after last solar minimum) is evaluated as follows:

$$H_{\mathrm{GCR}}(t) = w(t)\, H_{\mathrm{GCR}}^{\text{solar min}} + [1 - w(t)]\, H_{\mathrm{GCR}}^{\text{solar max}}$$

where $w(t)$ is the modulation function value (fig. 3) and $H_{\mathrm{GCR}}^{\text{solar min}}$ and $H_{\mathrm{GCR}}^{\text{solar max}}$ are the GCR doses listed in tables 3 to 6. Figures 13 and 14 illustrate the GCR dose-equivalent variations during the 11-year solar cycle that were calculated with this method. The ranges of the estimated skin and BFO doses are shown for both the low-density and the high-density atmosphere models at altitudes of 0 and 4 km.

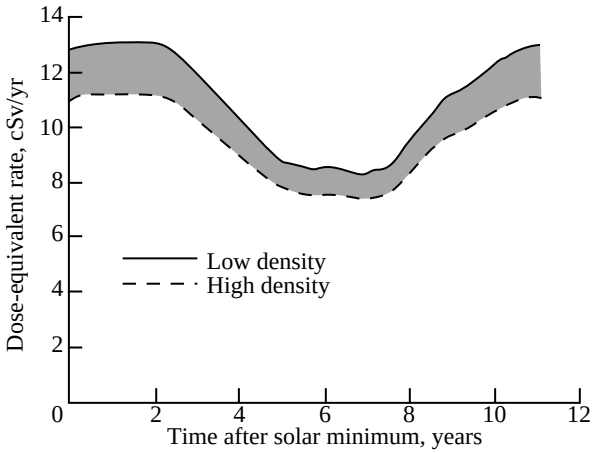

(a) Altitude = 0 km.

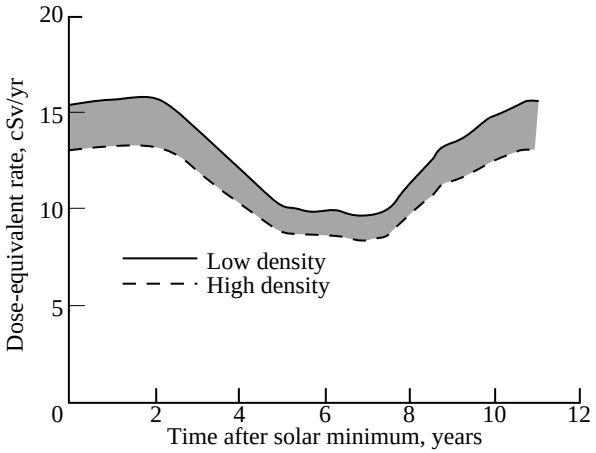

(b) Altitude = 4 km.

Figure 13. Annual skin dose-equivalent variation as a function of time in solar cycle for galactic cosmic radiation.

The surface doses incurred from GCR's for different Mars mission scenarios have been calculated. The references for the selected mission stay times are compiled in papers by Striepe, Nealy, and Simonsen (1992) and Striepe, Simonsen, and Nealy (1992). Table 7 shows the calculated doses for short-duration stay times on the Mars surface, and table 8 shows the calculated doses for long-duration stay times on the Mars surface. The GCR doses for a particular stay time are estimated by numerically integrating the curves of figures 13(a) and 14(a) between the Mars

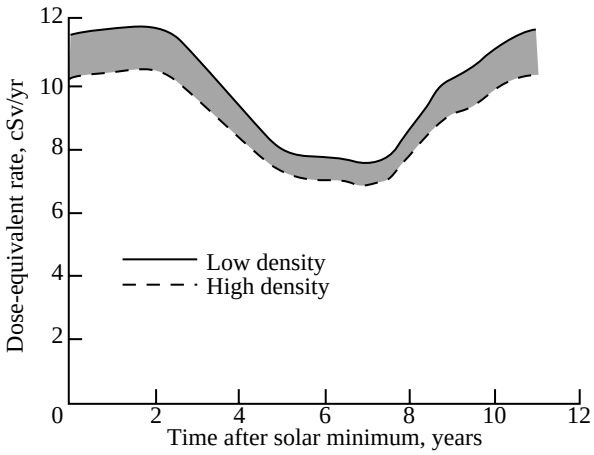

(a) Altitude = 0 km.

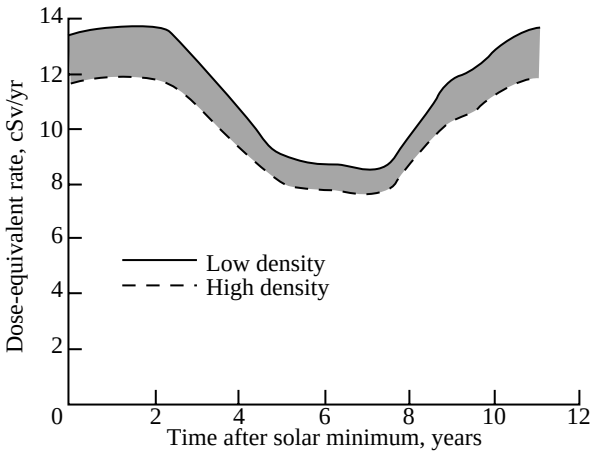

(b) Altitude = 4 km.

Figure 14. Annual BFO dose-equivalent variation as a function of time in solar cycle for galactic cosmic radiation.

arrival and departure dates. All calculations assume the stay is at an altitude of 0 km. (These calculations can be performed at other altitudes; however, the GCR dose does not vary significantly with altitude.) The calculations also assume that the crew member's only protection is the carbon dioxide atmosphere; i.e., the pressure vessel and other supporting equipment are not included as shielding. This approximation is only slightly conservative. Previous analyses have shown that moderate amounts of additional shielding will not provide substantial additional protection over that already provided by the atmosphere (Simonsen et al. 1990b).

For illustrative purposes, the surface doses of table 7 can be compared with the LEO limits; however, the doses incurred for the entire mission must remain below the limits. (However, the LEO limits can differ from future limits or acceptable risks established by the NCRP for exploratory missions.) The estimated GCR doses for surface stays of 30 days do not contribute significantly to the 25-cSv BFO or to the 150-cSv skin limits; likewise, the GCR doses for short-duration missions over 30 days do not contribute significantly to the yearly skin and BFO limits of 300 cSv and 50 cSv, respectively. Similarly for the long-duration missions lasting over a year, the GCR doses listed in table 8 do not surpass the yearly skin or BFO limits.

The other main contributor to dose that should be considered is the dose from a large solar flare event. Tables 7 and 8 list the arrival and departure dates in terms of years after the last solar minimum. For missions during active solar conditions (≈years 3–9), the occurrence of a large solar proton event can be considered. The 1989 large flare environment can be assumed or one of the large flares of August 1972, November 1960, and February 1956 can be assumed. (The doses for these flares are listed in Simonsen et al. 1990a.) The September 29 flare occurred approximately 48 days after the August 12 flare, and the October 19 flare occurred approximately 20 days after the September event. While on the surface of Mars, the 1989 flares do not individually contribute significantly toward the 30-day BFO and skin limits (assuming LEO limits) of 25 cSv and 150 cSv, respectively. The September and October doses can be added together and compared with the 30-day limit because they occur approximately 20 days apart. The sum of the September and October BFO doses of approximately 2.2 cSv to 4.7 cSv (tables 4 and 6) also does not contribute significantly toward the 30-day limits.

Combining the doses from three flare events with the estimated GCR dose during a time of active solar conditions can be appropriate for missions lasting approximately 70 days or more, or as previously illustrated, two events can be combined for missions with stay times between 30 and 50 days. For example, mission 1 of table 7 lasted 100 days and occurred during year 6 of the solar cycle (solar maximum conditions). An estimated total BFO dose for the surface stay can be on the order of 4.2 cSv to 7.1 cSv from both galactic cosmic rays and solar flare events. A BFO dose of 4.2 cSv is estimated from the high-density results of 1.9 cSv from GCR's (table 7) plus the sum of the 1989 solar flare doses of 0.1 cSv, 1.0 cSv, and 1.2 cSv (table 4). Likewise, a BFO dose of 7.1 is estimated from the low-density results of 2.1 cSv from GCR's (table 7) plus the sum of the 1989 solar flare doses of 0.3 cSv, 2.0 cSv, and

Table 7. Estimated GCR Dose for Short-Duration Stays on Surface

Mission	Arrival		Departure		Stay time (days)	Dose equivalent, cSv			
						Skin		BFO	
	Date	Yr. after solar min.	Date	Yr. after solar min.		High density	Low density	High density	Low density
1	7/11/2014	6.7	10/19/2014	6.9	100	2.1	2.3	1.9	2.1
2	2/15/2008	0.3	3/26/2008	0.4	40	1.2	1.4	1.1	1.3
3	7/1/2014	6.6	9/29/2014	6.9	90	1.9	2.1	1.7	1.9
4	11/18/2020	2.1	12/18/2020	2.2	30	0.9	1.1	0.9	1.0
5	8/4/2016	8.7	9/23/2016	8.9	50	1.4	1.6	1.3	1.4
6	9/27/2011	3.9	10/27/2011	4.0	30	0.8	0.9	0.7	0.8
7	4/11/2005	8.3	5/11/2005	8.4	30	0.8	0.9	0.7	0.8
8	3/24/2018	10.4	5/23/2018	10.5	60	1.9	2.2	1.7	2.0
9	2/26/2018	10.3	4/27/2018	10.5	60	1.8	2.2	1.7	1.9
10	6/11/2024	5.7	8/10/2024	5.8	60	1.3	1.4	1.2	1.3
11	7/13/2018	10.7	9/11/2018	10.8	60	1.9	2.2	1.7	2.0
12	8/27/2014	6.8	9/26/2014	6.9	30	0.6	0.7	0.6	0.6

Table 8. Estimated GCR Dose for Long-Duration Stays on Surface

Mission	Arrival		Departure		Stay time (days)	Dose equivalent, cSv			
						Skin		BFO	
	Date	Yr. after solar min.	Date	Yr. after solar min.		High density	Low density	High density	Low density
1	3/17/2008	0.3	10/15/2009	1.9	577	17.9	20.9	16.7	18.9
2	6/10/2008	0.6	8/21/2009	1.8	437	13.6	15.9	12.6	14.3
3	4/29/2010	2.5	11/18/2011	4.0	568	15.7	18.1	14.5	16.4
4	8/13/2010	2.7	8/22/2011	3.8	374	10.3	11.9	9.6	10.8
5	6/1/2012	4.5	10/26/2013	6.0	512	11.1	12.5	10.2	11.3
6	6/4/2012	4.6	12/21/2013	6.0	565	12.2	13.7	11.3	12.5
7	7/1/2014	6.6	3/11/2016	8.3	619	13.8	15.6	12.8	14.1
8	8/29/2014	6.8	11/30/2015	8.0	458	10.0	11.3	9.3	10.3
9	8/31/2016	8.8	5/3/2018	10.5	610	17.7	20.6	16.5	18.6
10	10/1/2016	8.9	3/14/2018	10.3	529	15.3	17.8	14.3	16.1
11	10/1/2018	10.9	8/8/2020	1.8	677	21.2	24.7	19.7	22.3
12	1/7/2019	0.2	6/6/2020	1.7	516	16.0	18.7	14.9	16.9
13	12/12/2020	2.2	9/16/2022	3.9	643	18.1	21.0	16.9	19.0
14	2/19/2021	2.4	7/21/2022	3.8	517	14.6	16.9	13.5	15.3

2.7 cSv (table 6). (For conservatism, this example does not apply the $1/r^2$ factor to the solar flare doses.) Flare doses can also be added to the GCR doses for other missions as deemed appropriate. For the long-duration missions, for instance, it would be appropriate to add the 1989 flare doses (or one of the other large flare doses) to the GCR dose for missions during active Sun conditions.

The doses incurred during transit to and from Mars will most likely dominate the total mission dose (Nealy et al. 1991). The surface dose estimates presented here have been incorporated into the MIRACAL program, which can be used to estimate doses for an entire Mars mission, including transit to and from Earth (Nealy, Striepe, and Simonsen 1992). Applications of the MIRACAL code for various Mars missions including surface stay doses are presented in the work of Striepe, Nealy, and Simonsen (1992) and Striepe, Simonsen, and Nealy (1992).

Concluding Remarks

The Mars surface doses presented here for the 1989 flares and the galactic cosmic rays (GCR's) during solar maximum conditions can be used in conjunction with previously estimated doses to estimate surface doses for a variety of Mars mis-

sion scenarios. The surface doses are an important consideration in planning a complete mission that requires dose estimates for each phase of the mission to determine crew-shielding requirements. Within the context of present radiation environment models and conventional dosimetry, long-term exposures to astronauts while on the Martian surface largely are shown to remain well below prescribed Space Station *Freedom* exposure limits. The protection is assumed to be provided solely by the atmosphere and planetary shadowing.

The estimated GCR annual exposures to blood-forming organs range from 6 to 12 cSv for solar maximum and solar minimum conditions, respectively, at the Mars datum altitude of 0 km (sea level). At an altitude of 12 km, these doses increase by approximately 15 percent. For the present analysis, the only circumstances for which short-term (1-month) and annual exposure limits are approached or exceeded occur when large solar proton events deliver exposures at high altitudes (10–12 km). In these cases, some additional provisional shielding is required.

The calculated exposure data for galactic cosmic rays and solar proton events have been generated in terms of the pertinent parameters altitude, solar cycle modulation factor, and high- and low-density model atmospheres. The data have been incorporated into a Mars mission dose prediction algorithm that can be applied to a wide variety of scenarios. As has been demonstrated herein, the data are particularly useful in providing realistic projections and associated ranges of exposures during Mars missions that feature relatively long-duration surface stay times.

NASA Langley Research Center
Hampton, VA 23681-0001
December 8, 1992

References

Adams, J. H., Jr.; Silberberg, R.; and Tsao, C. H. 1981: *Cosmic Ray Effects on Microelectronics. Part I—The Near-Earth Particle Environment.* NRL Memo. Rep. 4506-Pt. I, U.S. Navy, Aug. (Available from DTIC as AD A103 897.)

Anon. 1975: *Interplanetary Charged Particles.* NASA Space Vehicle Design Criteria (Environment). NASA SP-8118, 1975.

Anon. 1987: *Recommendations of the International Commission on Radiological Protection.* ICRP Publ. 26, Pergamon Press, c.1987.

Anon. 1989: *Guidance on Radiation Received in Space Activities.* NCRP Rep. No. 98, July 31, 1989.

Cucinotta, Francis A.; Katz, Robert; Wilson, John W.; Townsend, Lawrence W.; Shinn, Judy; and Hajnal, Ferenc 1991: Biological Effectiveness of High-Energy Protons—Target Fragmentation. *Radiat. Res.,* vol. 127, pp. 130–137.

Hess, S. L.; Ryan, J. A.; Tillman, J. E.; Henry, R. M.; and Leovy, C. B. 1980: The Annual Cycle of Pressure on Mars Measured by Viking Landers 1 and 2. *Geophys. Res. Lett.,* vol. 7, no. 3, Mar., pp. 197–200.

Nealy, J. E.; Simonsen, L. C.; and Striepe, S. A. 1992: Natural Radiation Environment Fluence and Dose Predictions for Missions to the Moon and Mars. *Proceedings of the Topical Meeting on New Horizons in Radiation Protection and Shielding,* American Nuclear Soc., Inc., pp. 181–187.

Nealy, John E.; Simonsen, Lisa C.; Wilson, John W.; Townsend, Lawrence W.; Qualls, Garry D.; Schnitzler, Bruce G.; and Gates, Michele M. 1991: Radiation Exposure and Dose Estimates for a Nuclear-Powered Manned Mars Sprint Mission. *Proceedings of the Eighth Symposium on Space Nuclear Power Systems, Part Two,* Mohamed S. El-Genk and Mark D. Hoover, eds., CONF-910116, American Inst. of Physics, pp. 531–536.

Nealy, John E.; Striepe, Scott A.; and Simonsen, Lisa C. 1992: *MIRACAL: A Mission Radiation Calculation Program for Analysis of Lunar and Interplanetary Missions.* NASA TP-3211.

Sauer, Herbert H.; Zwickl, Ronald D.; and Ness, Martha J. 1990: *Summary Data for the Solar Energetic Particle Events of August Through December 1989.* Space Environment Lab., National Oceanic and Atmospheric Adm., Feb. 21.

Simonsen, Lisa C.; and Nealy John E. 1991: *Radiation Protection for Human Missions to the Moon and Mars.* NASA TP-3079.

Simonsen, Lisa C.; Nealy, John E.; Townsend, Lawrence W.; and Wilson, John W. 1990a: *Radiation Exposure for Manned Mars Surface Missions.* NASA TP-2979.

Simonsen, Lisa C.; Nealy, John E.; Townsend, Lawrence W.; and Wilson, John W. 1990b: Space Radiation Shielding for a Martian Habitat. SAE Tech. Paper Ser. 901346, July.

Smart, D. F.; and Shea, M. A. 1989: Solar Proton Events During the Past Three Solar Cycles. *J. Spacecr. & Rockets,* vol. 26, no. 6, Nov.–Dec., pp. 403–415.

Smith, Robert E.; and West, George S., compilers 1983: *Space and Planetary Environment Criteria Guidelines for Use in Space Vehicle Development, 1982 Revision (Volume 1).* NASA TM-82478.

Striepe, Scott A.; Nealy, John E.; and Simonsen, Lisa C. 1992: Radiation Exposure Predictions for Short-Duration-Stay Mars Missions. Paper AAS 92-107, Feb.

Striepe, Scott A.; Simonsen, Lisa C.; and Nealy, John E. 1992: Radiation Exposure for Long-Duration-Stay Mars Missions. AIAA-92-4584, Aug.

Švestka, Zdeněk c.1976: *Solar Flares.* D. Reidel Publ. Co., Inc.

Townsend, Lawrence W.; Cucinotta, Francis A.; and Wilson, John W. 1992: Interplanetary Crew Exposure Estimates for Galactic Cosmic Rays. *Radiat. Res.,* vol. 129, no. 1, pp. 48–52.

Townsend, Lawrence W.; Nealy, John E.; Wilson, John W.; and Atwell, William 1989: Large Solar Flare Radiation Shielding Requirements for Manned Interplanetary Missions. *J. Spacecr. & Rockets,* vol. 26, Mar.–Apr., pp. 126–128.

Townsend, Lawrence W.; Shinn, Judy L.; and Wilson, John W. 1991: Interplanetary Crew Exposure Estimates for the August 1972 and October 1989 Solar Particle Events. *Radiat. Res.,* vol. 126, pp. 108–110.

Townsend, L. W.; Wilson, J. W.; Shinn, J. L.; and Curtis, S. B. 1992: Human Exposure to Large Solar Particle Events in Space. *Adv. Space Res.,* vol. 12, no. 2–3, pp. (2)339–(2)348.

Wilson, John W.; Chun, Sang Y.; Badavi, Forooz F.; Townsend, Lawrence W.; and Lamkin, Stanley L. 1991a: *HZETRN: A Heavy Ion-Nucleon Transport Code for Space Radiations.* NASA TP-3146.

Wilson, John W.; Townsend, Lawrence W.; Nealy, John E.; Chun, Sang Y.; Hong, B. S.; Buck, Warren W.; Lamkin, S. L.; Ganapol, Barry D.; Khan, Ferdous; and Cucinotta, Francis A. 1989: *BRYNTRN: A Baryon Transport Model.* NASA TP-2887.

Wilson, John W.; Townsend, Lawrence W.; Schimmerling, Walter; Khandelwal, Govind S.; Khan, Ferdous; Nealy, John E.; Cucinotta, Francis A.; Simonsen, Lisa C.; Shinn, Judy L.; and Norbury, John W. 1991b: *Transport Methods and Interactions for Space Radiations.* NASA RP-1257.

Withbroe, George L. 1989: Solar Activity Cycle: History and Predictions. *J. Spacecr. & Rockets,* vol. 26, no. 6, Nov.–Dec., pp. 394–402.

REPORT DOCUMENTATION PAGE

Form Approved
OMB No. 0704-0188

1. AGENCY USE ONLY *(Leave blank)*	2. REPORT DATE	3. REPORT TYPE AND DATES COVERED
	February 1993	Technical Paper

4. TITLE AND SUBTITLE
Mars Surface Radiation Exposure for Solar Maximum Conditions and 1989 Solar Proton Events

5. FUNDING NUMBERS
WU 593-42-31-01

6. AUTHOR(S)
Lisa C. Simonsen and John E. Nealy

7. PERFORMING ORGANIZATION NAME(S) AND ADDRESS(ES)
NASA Langley Research Center
Hampton, VA 23681-0001

8. PERFORMING ORGANIZATION REPORT NUMBER
L-17152

9. SPONSORING/MONITORING AGENCY NAME(S) AND ADDRESS(ES)
National Aeronautics and Space Administration
Washington, DC 20546-0001

10. SPONSORING/MONITORING AGENCY REPORT NUMBER
NASA TP-3300

11. SUPPLEMENTARY NOTES

12a. DISTRIBUTION/AVAILABILITY STATEMENT
Unclassified–Unlimited

Subject Category 93

12b. DISTRIBUTION CODE

13. ABSTRACT *(Maximum 200 words)*

The Langley heavy-ion/nucleon transport code, HZETRN, and the high-energy nucleon transport code, BRYNTRN, are used to predict the propagation of galactic cosmic rays (GCR's) and solar flare protons through the carbon dioxide atmosphere of Mars. Particle fluences and the resulting doses are estimated on the surface of Mars for GCR's during solar maximum conditions and the August, September, and October 1989 solar proton events. These results extend previously calculated surface estimates for GCR's at solar minimum conditions and the February 1956, November 1960, and August 1972 solar proton events. Surface doses are estimated with both a low-density and a high-density carbon dioxide model of the atmosphere for altitudes of 0, 4, 8, and 12 km above the surface. A solar modulation function is incorporated to estimate the GCR dose variation between solar minimum and maximum conditions over the 11-year solar cycle. By using current Mars mission scenarios, doses to the skin, eye, and blood-forming organs are predicted for short- and long-duration stay times on the Martian surface throughout the solar cycle.

14. SUBJECT TERMS	15. NUMBER OF PAGES
Mars atmosphere; Solar proton events; Mars missions; Galactic cosmic radiation; Dose	14
	16. PRICE CODE A03

17. SECURITY CLASSIFICATION OF REPORT	18. SECURITY CLASSIFICATION OF THIS PAGE	19. SECURITY CLASSIFICATION OF ABSTRACT	20. LIMITATION OF ABSTRACT
Unclassified	Unclassified		

NSN 7540-01-280-5500

Standard Form 298(Rev. 2-89)
Prescribed by ANSI Std. Z39-18
298-102